Advances in Nano Research, *Vol. 14, No. 5 (2023) 421-433*
https://doi.org/10.12989/anr.2023.14.5.421

The influence of non-linear carbon nanotube reinforcement on the natural frequencies of composite beams

Mehmet Avcar*[1], Lazreg Hadji[2,3] and Ömer Civalek[4,5]

[1]*Department of Civil Engineering, Faculty of Engineering, Suleyman Demirel University, Isparta, Turkey*
[2]*Faculty of Civil Engineering, Ton Duc Thang University, Ho Chi Minh City 70000, Vietnam*
[3]*Laboratory of Geomatics and Sustainable Development, University of Tiaret, Algeria*
[4]*Department of Medical Research, China Medical University Hospital, China Medical University, Taichung, Taiwan*
[5]*Civil Engineering Department, Akdeniz University, Antalya, Turkey*

(*Received April 21, 2022, Revised August 23, 2022, Accepted September 14, 2022*)

Abstract. In the present paper, the influences of the variation of exponent of volume fraction of carbon nanotubes (CNTs) on the natural frequencies (NFs) of the carbon nanotube-reinforced composite (CNTRC) beams under four different boundary conditions (BCs) are investigated. The single-walled carbon nanotubes (SWCNTs) are assumed to be aligned and dispersed in a polymeric matrix with various reinforcing patterns, according to the variation of exponent of volume fraction of CNTs for functionally graded (FG) reinforcements. Besides, uniform distribution (UD) of reinforcement is also considered to analyze the influence of the non-linear (NL) variation of the reinforcement of CNTs. Using Hamilton's principle and third-order shear deformation theory (TSDT), the equations of motion of the CNTRC beam are derived. Under four different BCs, the resulting equations are solved analytically. To verify the present formulation, comparison investigations are conducted. To examine the impacts of several factors on the NFs of the CNTRC beams, numerical examples and some benchmark results are presented.
Keywords: closed-form solution; CNTRC beams; natural frequency; non-linear reinforcement; TSDT

1. Introduction

The use of non-uniform, non-homogeneous, and reinforced components helps meet the standards such as safety, usefulness, aesthetics, and affordability which are all desired characteristics of structural components in engineering applications while also minimizing total cost and weight. Any solid with more than one component, such as in different phases is referred to as a composite material. The distinctive characteristics of composite materials stem from the interaction of these components. Numerous historical examples of composites exist in the open literature, and their first use dates to 1500 BC. Mud walls reinforced by bamboo in the houses of Egyptians, glued laminated boards, and laminated metals in forged swords in 1800 BC are some examples. Today, composite materials are of several types, such as glass fiber–reinforced aluminium, carbon-reinforced fiber plastic, composites with carbon nanotubes, as well as composites including metal-matrix or ceramic-matrix, etc. and they have a wide variety of applications in several fields of recent engineering, as, aerospace, automotive, aviation, civil, defence, marine, mechanical, among others (Reddy 2003, Kaw 2006, Vinson and Sierakowski 2008).

Allotropes of carbon having long, narrow cylinders are called CNTs and were discovered by Iijima (1991). CNTs are constructed of graphite and have a tubular form (Lau and Hui 2002, Lau *et al*. 2004, Ramezani *et al*. 2022). The outside diameter of the tubes, which varied from around 3 nm to 30 nm, had at least two layers and sometimes many more (Loos 2014, Saifuddin *et al*. 2013, Liew *et al*. 2015). CNTs are massive macromolecules that are distinctive due to their size, shape, and exceptional mechanical and physical characteristics, i.e., CNTs can have a length-to-diameter ratio greater than 1,000,000, and they are known as the strongest and stiffest materials yet discovered in terms of tensile strength and elastic modulus, respectively. (Esawi and Farag 2007, Barretta *et al*. 2019, Feng *et al*. 2021, Ramezani *et al*. 2021). As a result, CNTs have been used as reinforcing components instead of conventional composites to construct high-performance structural and multifunctional composites nowadays. (Ehyaei and Daman 2017, Rashad 2017, Khadimallah *et al*. 2021, Khadir *et al*. 2021,). Thus, understanding the mechanical behaviour of nanostructures is hence of tremendous interest, and so experimental and computer simulation approaches such as molecular dynamics (MD) modelling and classical continuum mechanics might be employed to achieve this goal. Among these approaches, classical continuum mechanics is the most extensively used by researchers because of its computational simplicity and efficacy, as well as nanoscale experimental research is challenging and time-consuming, and the cost of MD simulations is quite expensive (Han and Elliott 2007, Tounsi *et al*. 2013, Hussain *et al*. 2020, Nejadi *et al*. 2021, Jalaei *et al*. 2022).

Researchers have been interested in the mechanical characteristics of structural elements, such as beams, plates, and shells reinforced by CNTs, for the last two decades.

*Corresponding author, Ph.D.,
E-mail: mehmetavcar@yahoo.com;
mehmetavcar@sdu.edu.tr

ISSN: 2287-237X (Print), 2287-2388 (Online)

Particularly, many studies have been performed to examine the static/dynamic behaviours of carbon nanotube-reinforced composite beams with constant and/or linear variation of the volume fraction of CNTs in the framework of several beam theories and considering varied factors. Mahmoodi *et al*. (2005) reported the NL vibration analysis of the CNTRC cantilever beam. Utilizing the first-order shear deformation theory (FSDT) of Timoshenko and von Kármán's geometric nonlinearity, Ke *et al*. (2010) examined NL free vibration of CNTRC beams. Chiroiu *et al*. (2010) established a mechanical model for multifunctional reinforced CNTRC beams by including couple stresses into the fundamental equations of the linear viscoelastic theory. Yas and Samadi (2012) examined the free vibration and buckling behaviours of CNTRC Timoshenko beams resting on elastic foundations. Deepak *et al*. (2012) examined the dynamics of uniform and tapered rotating CNTRC beams utilizing a spectral finite element model. Heshmati and Yas (2013) used an equivalent fiber based on the Eshelby-Mori-Tanaka technique to study the influence of CNTs aggregation and distribution on the free vibration characteristics of CNTRC beams. Shen and Xiang (2013) studied NL bending, vibration, and thermal post-buckling of CNTRC beams resting on an elastic foundation in thermal environments. Utilizing the FSDT of Timoshenko and von Kármán geometric nonlinearity, Ansari *et al*. (2014) investigated NL forced vibration of CNTRC beams. Based on FDST and TSDT, Lin and Xiang (2014a) analyzed the NL-free vibration of CNTRC beams employing the p-Ritz method. Mayandi and Jeyaraj (2015) used the FEM to investigate the mechanical behaviours of the CNTRC beam under varied non-uniform thermal loads. Heshmati *et al*. (2015) investigated the CNT length, waviness, agglomeration, and dispersion impacts on the vibration of CNTRC beams. Kamarian *et al*. (2016) presented the free vibration and optimization of CNTRC laminated beams based on various higher-order theories. Seidi and Kamarian (2017) examined the effects of nanotube volume fraction and agglomeration, long fiber volume fraction, and various layup schemes on the natural frequencies of non-uniform multi-scale CNTRC beams. Thomas and Suresh (2017) reported that the inclusion of CNTs and their arrangement plays an important effect on the elastic and dynamic features of the CNTRC beam. Mohammadimehr and Alimirzaei (2017) used the Finite Element Method (FEM) to investigate the buckling and free vibration of a tapered CNTRC micro-Reddy beam in a longitudinal magnetic field. Kumar and Srinivas (2017) conducted a computational investigation of the static and dynamic behaviours of CNTRC polymer and hybrid laminated beams. Applying FSDT, Shi *et al*. (2017) proposed an accurate approach to describe the free vibration of CNTRC beams with arbitrary BCs. Khilari (2018) used FEM to analyze the free vibration of CNTRC beams based on the FSDT of Timoshenko. Nejati *et al*. (2018) studied the natural frequencies of CNTRC thick beams made of randomly oriented agglomerated CNTs subjected to axial compressive force. Mahmoodi *et al*. (2018) used a 3D micromechanical model in conjunction with 2D elasticity macro mechanical theory to perform static and free vibration analyses of a CNTRC beam. Mohammadimehr *et al*. (2018) presented the results of the experimental tensile test and fabrication of the CNTRC beam and the mechanical behaviours of the CNTRC beam based on several theories. Using FEM and the FSDT, Duy *et al*. (2019) investigated the free vibration of laminated CNTRC beams. Borjalilou *et al*. (2019) used the FSDT of Timoshenko and the nonlocal elasticity theory to explore the mechanical behaviours of CNTRC nanobeams. Utilizing the FSDT of Timoshenko, Mohseni and Shakouri (2019) analyzed the free vibration and buckling of CNTRC beams with varying thicknesses resting on elastic foundations. Yang *et al*. (2020) studied the NL behaviour of temperature-dependent CNTRC laminated beams having variable CNT volume fractions in all layers and functional grading in the thickness direction with a piece-wise pattern. Afshin and Yas (2020) focused on the dynamic and buckling analyses of CNTRC beams having varying thickness that is concurrently reinforced with CNTs and nano clay. Bousahla *et al*. (2020) used an integral FSDT to analyze the dynamic and stability of a simply supported CNTRC beam resting on an elastic foundation. Mohammadimehr *et al*. (2020) utilized the modified couple stress theory to investigate the vibrations of a viscoelastic CNTRC microbeam. El-Ashmawy and Xu (2021) investigated the influence of CNT orientation and gradation distribution on static and free vibration analysis of CNTRC beams using FEM. Xu *et al*. (2021) examined the NFs of rotating Timoshenko CNTRC beams in thermal conditions with general BCs.

In addition, the mechanical responses of CNTRC structures having other geometries with constant and/or linear variations of the volume fraction of CNTs have also been reported by taking into account several higher-order theories and varied factors. In thermal environments, Shen (2009), and Wang and Shen (2011) analyzed the NL bending and vibration of CNTRC plates under simply supported BCs in thermal environments, respectively. Hedayati and Sobhani (2012) proposed a 3-D elasticity solution for the NFs of CNTRC annular sectorial plates resting on elastic foundations. Shen (2012) performed a thermal post-buckling analysis for CNTRC cylindrical shells exposed to a homogeneous temperature increase. Using the 3-D theory of elasticity, Alibeigloo and Emtahani (2015) studied the bending and free vibration of composite CNTRC plates. Jam and Kiani (2015) provided a lateral pressure-induced linear buckling study for CNTRC conical shells. Arani *et al*. (2016) analyzed the NL transverse vibration of an embedded piezoelectric plate reinforced with SWCNTs resting on a Pasternak foundation. Kamarian *et al*. (2016) conducted a free vibration study of CNTRC conical shells, considering the agglomeration effect of CNTs. Moradi-Dastjerdi (2017) examined the thermoelastic dynamic behaviour of FG-CNTRC cylinders subjected to mechanical pressure loads, uniform temperature environments, or thermal gradient loads utilizing a mesh-free method. Civalek and Baltacioglu (2018) addressed the modelling and numerical solution of free vibration problems of CNTRC annular and annular sector plates. Ansari *et al*. (2019) used the variational differential quadrature approach to analyze the free vibration of

embedded CNTRC conical, cylindrical, and annular plates. Rezaiee-Pajand *et al*. (2019) investigated the NL static and free vibration analysis of UD-CNTRC structures under in-plane loading. Bisheh *et al*. (2020) studied the impact of various boundary conditions and hygrothermal environmental effects on the free vibration of piezoelectric coupled CNTRC cylindrical shells. Civalek and Avcar (2020) used a four-nodded straight-sided transformation approach to investigate the mechanical behaviours of laminated quadrilateral and skew CNTRC plates. Chamran *et al*. (2022) investigated the dynamic instability in CNTRC plates exposed to periodic loadings.

Consequently, as a result of the detailed literature review, it has been highlighted that investigations of the mechanical responses of nano-composite structures reinforced by CNTs are constrained by the constant and/or linear variation of the volume fraction of CNTs, except for a few studies. For this context, Lin and Xiang (2014b) mentioned the NL variation of the volume fraction of CNTs. Zerrouki *et al*. (2020) and (2021) handled the influences of NL variation of volume fraction of CNTs on the buckling and bending responses of CNTRC beams, respectively. To the best of the authors' knowledge, the influence of the NL variation of volume fraction of CNTs on the natural frequencies (NFs) of CNTRC beams under different boundary conditions (BCs) has not been dealt with yet. Therefore, an attempt is made to address this problem in the current study. Distinct from the early studies on CNTRC structures, the rule of the mixture, including NL distribution of volume fraction of CNTs, is used to figure out the material properties of the CNTRC beams. The impacts of NL variation of CNT volume fraction, several types of CNT distribution patterns, span-to-depth ratio, and BCs on the natural frequencies of CNTRC beams are numerically simulated, and some benchmark results are presented.

The paper is arranged as follows. Section 2 is dedicated to defining the geometry and material properties of CNTRC beams. In Section 3, the governing equations of free vibration of CNTRC beams are found using Hamilton's principle and third-order shear deformation theory (TSDT). The analytical solution procedure of the present problem considering four different BCs is established in Section 4. Numerical results and discussions on the current problem are given in Section 5. Conclusions are finally drawn in Section 6.

2. The geometry and material properties of CNRC Beams

Let us assume a straight rectangular CNTRC beam of length L, width b, and thickness h along the x-,y-, and z-directions, respectively, where the Cartesian coordinate system is established on the left edge of the beam on the mid surface as shown in Fig. 1. CNTRC beam is supposed to be reinforced by the single-walled carbon nanotubes (SWCNTs) embedded in an isotropic polymer matrix, where the reinforcement in the thickness direction is assumed to have different Functionally Graded (FG) distribution patterns as FG-Λ, FG-O, and FG-X. Furthermore, Uniform Distribution (UD) reinforcement is

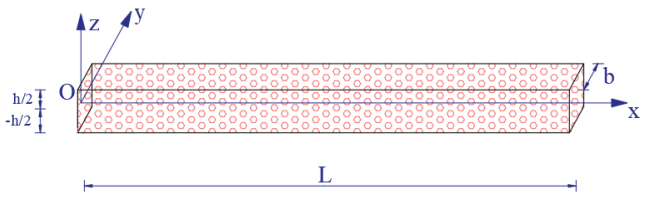

Fig. 1 The geometry of the CNTRC beam

also considered to analyze the influence of the NL variation of the reinforcement of CNTs. Since the density of CNTs within the area is constant, although the volume fraction varies as the beam thickness grows, there is no sudden interface between the CNTs and the polymer matrix along the beam. The illustrations of cross-sections relative to all patterns of CNTRC beam examined by varying the exponent of volume fraction are plotted in Fig. 2 (Zerrouki *et al*. 2020 and 2021). Here k is the exponent of the volume fraction of the CNTs, where $k = 0$ corresponds to UD, $k = 1$ corresponds to L dispersion, and $k \neq 1$ corresponds to the NL dispersion of CNTs in the matrix.

The volume fraction of CNTs, for different distribution patterns is defined as follows (Lin and Xiang 2008, Zerrouki *et al*. 2020, 2021):

$$\text{UD: } V_{cnt} = V_{cnt}^{*} \tag{1}$$

$$\text{FG-O: } V_{cnt} = (k+1)\left(1 - 2\frac{|z|}{h}\right)^{k} V_{cnt}^{*} \tag{2}$$

$$\text{FG-X: } V_{cnt} = (k+1)\left(2\frac{|z|}{h}\right)^{k} V_{cnt}^{*} \tag{3}$$

$$\text{FG-}\Lambda\text{: } V_{cnt} = (k+1)\left(\frac{1}{2} - \frac{z}{h}\right)^{k} V_{cnt}^{*} \tag{4}$$

$$\text{FG-V: } V_{cnt} = (k+1)\left(\frac{1}{2} + \frac{z}{h}\right)^{k} V_{cnt}^{*} \tag{5}$$

where V_{cnt}^{*} is the specified volume fraction of CNTs and given by:

$$V_{cnt}^{*} = \frac{W_{cnt}}{W_{cnt} + (\rho^{cnt}/\rho^{m})(1 - W_{cnt})} \tag{6}$$

being W_{cnt}, ρ^{cnt}, and ρ^{p} the mass fraction and density of CNTs, and the density of polymer matrix, respectively.

By matching molecular dynamics simulation findings, depending on the mixture rule, the efficient Young's and shear modulus of CNTRC beams may be calculated as follows:

$$E_{11} = \eta_1 V_{cnt} E_{11}^{cnt} + V_p E^{p} \tag{7}$$

$$\frac{\eta_2}{E_{22}} = \frac{V_{cnt}}{E_{22}^{cnt}} + \frac{V_p}{E^{p}} \tag{8}$$

$$\frac{\eta_3}{G_{12}} = \frac{V_{cnt}}{G_{12}^{cnt}} + \frac{V_p}{G^{p}} \tag{9}$$

$$V_{cnt} + V_p = 1 \tag{10}$$

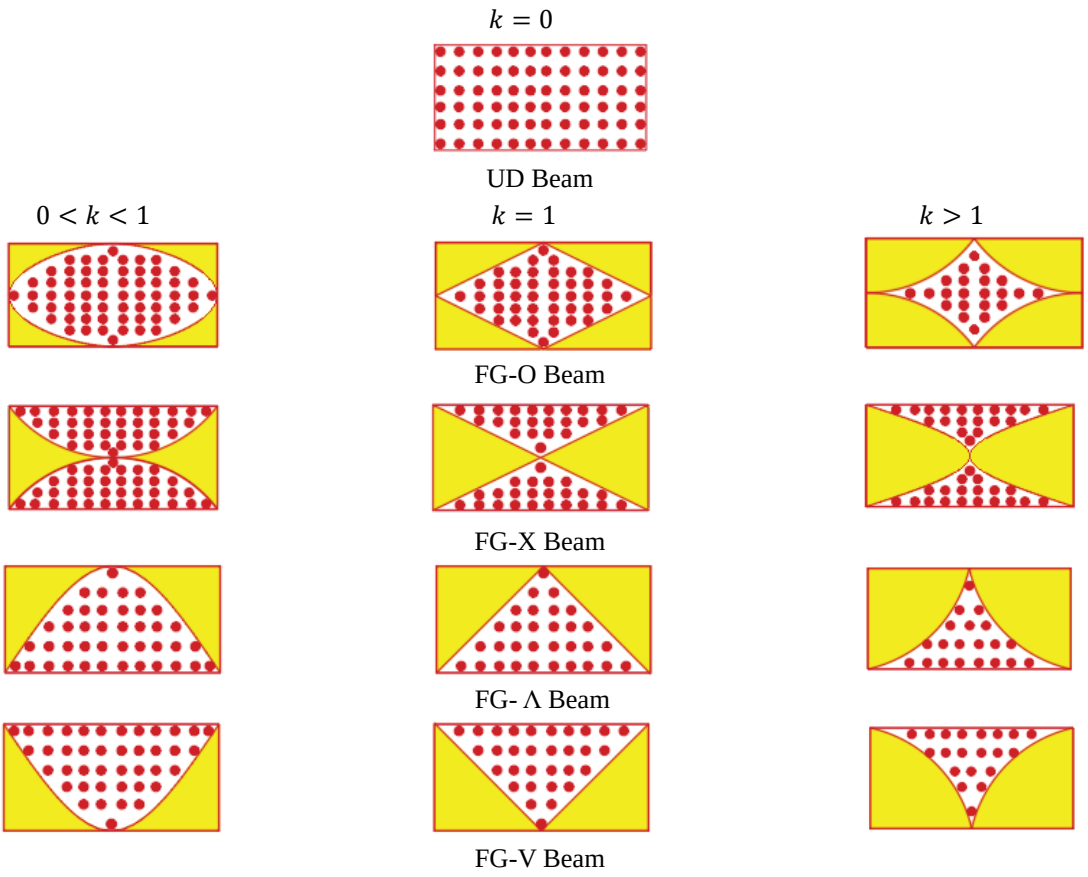

Fig. 2 Cross-sections of UD, FG-O, FG-Λ, and FG-V patterns of the CNTRC beam for different values of volume fraction index

where E^p and G^p are Young's modulus and shear modulus of the polymer matrix, V_{cnt} and V_p are the volume fractions of CNTs and the polymer matrix, respectively, and E_{11}^{cnt}, E_{22}^{cnt} and G_{12}^{cnt} are Young's and shear modulus of SWCNTs, respectively.

Correspondingly, the Poisson's ratio (ν) and density (ρ) of the CNTRC beam may be given as:

$$\nu = V_{cnt}\nu^{cnt} + V_p\nu^p \tag{11}$$

$$\rho = V_{cnt}\rho^{cnt} + V_p\rho^p \tag{12}$$

where ν^{cnt}, ν^p and ρ^{cnt}, ρ^p are the Poisson's ratio and density of the CNTs and polymer matrix, respectively.

3. Governing equations

3.1 Fundamental assumptions

In this subsection, the adopted assumptions of the present theory are detailed. The middle surface of the CNTRC beam is supposed to be located at the origin of the coordinate system. Since the displacements are small concerning the height of the CNTRC beam, the stresses concerned are neglected. Moreover, the transverse displacement is considered to be composed of bending and shear that are solely functions of the *x* and *t* as:

$$w(x,z,t) = w_b(x,t) + w_s(x,t) \tag{13}$$

Compared to in-plane stress, σ_x, the transverse normal stress σ_z is presumed to be negligible. Normal, bending, and shear components are supposed to comprise the axial displacement, u, in the *x*-direction. Then, the axial displacement, u, in the x-direction is made up of normal, bending, and shear components:

$$u = u_0 + u_b + u_s \tag{14}$$

The bending displacement component w_b can be found according to the classical beam theory and so u_b is defined as follow:

$$u_b = -z\frac{\partial w_b}{\partial x} \tag{15}$$

The shear displacement components u_s and w_s cause the hyperbolic changing of shear strain γ_{xz} and so shear stress, τ_{xz}, is zero at the top and bottom of the CNTRC beam. Thus, u_s is as follows:

$$u_s = -f(z)\frac{\partial w_s}{\partial x} \tag{16}$$

where to fulfil the stress-free BCs on the top and bottom of the CNTRC beam, the shape function $f(z)$ is chosen using TSDT as follows (Benachour *et al*. 2011):

$$f(z) = z\left[-\frac{1}{4} + \frac{5}{3}\left(\frac{z}{h}\right)^2\right] \tag{17}$$

3.2 Kinematics and constitutive relations

The displacement field of the third-order refined beam theory may be calculated using Eqs. (13)-(17) as a function of the assumptions established in section 3.1., that is:

$$u(x,z,t) = u_0(x,t) - z\frac{\partial w_b}{\partial x} - f(z)\frac{\partial w_s}{\partial x} \tag{18}$$

$$w(x,z,t) = w_b(x,t) + w_s(x,t) \tag{19}$$

The strains related to the displacements are:

$$\varepsilon_x = \varepsilon_x^0 + z\,k_x^b + f(z)\,k_x^s \tag{20}$$

$$\gamma_{xz} = g(z)\,\gamma_{xz}^s \tag{21}$$

where

$$\varepsilon_x^0 = \frac{\partial u_0}{\partial x},\ k_x^b = -\frac{\partial^2 w_b}{\partial x^2},\ k_x^s = -\frac{\partial^2 w_s}{\partial x^2},\ \gamma_{xz}^s = \frac{\partial w_s}{\partial x} \tag{22}$$

$$g(z) = 1 - \frac{df(z)}{dz} \tag{23}$$

By assuming that the CNTRC beam obeys Hooke's law, the stresses are expressed as:

$$\sigma_x = Q_{11}(z)\,\varepsilon_x \tag{24}$$

$$\tau_{xz} = Q_{55}(z)\,\gamma_{xz} \tag{25}$$

where

$$Q_{11}(z) = \frac{E_{11}(z)}{1-\nu^2};\ Q_{55}(z) = G_{12}(z) \tag{26}$$

Being $E_{11}(z)$ and $G_{12}(z)$ are the effective Young's and shear modulus of CNTRC beams.

$$E_{xx} = -y_l\frac{\partial^2 w(x_l,t)}{\partial x^2} \tag{27}$$

3.3 Equations of motion

In the present study, the equations of motion are developed by using Hamilton's principle (Reddy 2003a, b):

$$\int_{t_1}^{t_2}(\delta U - \delta T)\,dt = 0 \tag{28}$$

where t, t_1, and t_2 are time, the initial, and end time, correspondingly, δU is the virtual change of the strain energy and δT is the virtual change of the kinetic energy.

The change strain energy of the CNTRC beam may be expressed as

$$\begin{aligned}\delta U &= \int_0^L\int_{-\frac{h}{2}}^{\frac{h}{2}}(\sigma_x\delta\,\varepsilon_x + \tau_{xz}\delta\,\gamma_{xz})dzdx \\ &= \int_0^L\left(N_x\frac{\partial\delta\,u_0}{\partial x} - M_x^b\frac{\partial^2\delta\,w_b}{\partial x^2} - M_x^s\frac{\partial^2\delta\,w_s}{\partial x^2}\right. \\ &\qquad \left. + Q_{xz}\frac{\partial\delta\,w_s}{dx}\right)dx\end{aligned} \tag{29}$$

where N_x, M_x^b, M_x^s and Q_{xz} are the stress resultants computed as:

$$\begin{aligned}(N_x, M_x^b, M_x^s) &= \int_{-\frac{h}{2}}^{\frac{h}{2}}(1, z, f(z))\,\sigma_x dz \\ \text{and } Q_{xz} &= \int_{-\frac{h}{2}}^{\frac{h}{2}} g(z)\tau_{xz}dz\end{aligned} \tag{29}$$

where $f(z)$ and $g(z)$ are shape functions.

The change in kinetic energy of the CNTRC beam can be stated in the following way:

$$\begin{aligned}\delta\,T &= \int_0^L\int_{-\frac{h}{2}}^{\frac{h}{2}}\rho(z)[\dot{u}\delta\,\dot{u} + \dot{w}\delta\,\dot{w}]\,dzdx \\ &= \int_0^L\left\{I_0[\dot{u}_0\delta\dot{u}_0 + (\dot{w}_b+\dot{w}_s)(\delta\dot{w}_b+\delta\dot{w}_s)]\right. \\ &\qquad - I_1\left(\dot{u}_0\frac{\partial\delta\dot{w}_b}{\partial x} + \frac{\partial\dot{w}_b}{\partial x}\delta\,\dot{u}_0\right) \\ &\quad + I_2\left(\frac{\partial\dot{w}_b}{\partial x}\frac{\partial\delta\,\dot{w}_b}{\partial x}\right) - J_1\left(\dot{u}_0\frac{\partial\delta\dot{w}_s}{\partial x} + \frac{\partial\dot{w}_s}{\partial x}\delta\,\dot{u}_0\right) \\ &\quad \left. + K_2\left(\frac{d\dot{w}_s}{\partial x}\frac{\partial\delta\,\dot{w}_s}{\partial x}\right) + J_2\left(\frac{\partial\dot{w}_b}{\partial x}\frac{\partial\delta\,\dot{w}_s}{\partial x} + \frac{\partial\dot{w}_s}{\partial x}\frac{\partial\delta\,\dot{w}_b}{\partial x}\right)\right\}dx\end{aligned} \tag{30}$$

here the dot-superscript convention represents differentiation concerning time, $\rho(z)$ is the mass density, and $(I_0,\ I_1,\ J_1,\ I_2,\ J_2,\ K_2)$ are the mass moment of inertias given by:

$$(I_0, I_1, J_1, I_2, J_2, K_2) = \int_{-\frac{h}{2}}^{\frac{h}{2}}(1, z, f, z^2, zf, f^2)\rho(z)dz \tag{31}$$

Substituting Eqs. (28) and (30) into Eq. (27), then collecting together the coefficients of $\delta\,u_0$, $\delta\,w_b$, and $\delta\,w_s$, and at last integrating by components versus both spatial and time variables, the following equations of motion of CNTRC beam are obtained:

$$\delta\,u_0\text{:}\quad \frac{\partial N_x}{\partial x} = I_0\ddot{u}_0 - I_1\frac{\partial\ddot{w}_b}{\partial x} - J_1\frac{\partial\ddot{w}_s}{\partial x} \tag{32}$$

$$\begin{aligned}&\delta\,w_b\text{:}\quad \frac{\partial^2 M_b}{\partial x^2} \\ &= I_0(\ddot{w}_b+\ddot{w}_s) + I_1\frac{\partial\ddot{u}_0}{\partial x} - I_2\frac{\partial^2\ddot{w}_b}{\partial x^2} - J_2\frac{\partial^2\ddot{w}_s}{\partial x^2}\end{aligned} \tag{33}$$

$$\begin{aligned}&\delta\,w_s\text{:}\quad \frac{\partial^2 M_s}{\partial x^2} + \frac{\partial Q_{xz}}{\partial x} \\ &= I_0(\ddot{w}_b+\ddot{w}_s) + J_1\frac{\partial\ddot{u}_0}{\partial x} - J_2\frac{\partial^2\ddot{w}_b}{\partial x^2} - K_2\frac{\partial^2\ddot{w}_s}{\partial x^2}\end{aligned} \tag{34}$$

Eqs. (32)-(34) can be expressed in terms of displacements (u_0, w_b, w_s) by using Eqs. (20)-(23), (24)-(26), and (29) as follows:

$$\begin{aligned}&A_{11}\frac{\partial^2 u_0}{\partial x^2} - B_{11}\frac{\partial^3 w_b}{\partial x^3} - B_{11}^s\frac{\partial^3 w_s}{\partial x^3} \\ &= I_0\ddot{u}_0 - I_1\frac{\partial\ddot{w}_b}{\partial x} - J_1\frac{\partial\ddot{w}_s}{\partial x}\end{aligned} \tag{35}$$

$$\begin{aligned}&B_{11}\frac{\partial^3 u_0}{\partial x^3} - D_{11}\frac{\partial^4 w_b}{\partial x^4} - D_{11}^s\frac{\partial^4 w_s}{\partial x^4} \\ &= I_0(\ddot{w}_b+\ddot{w}_s) + I_1\frac{\partial\ddot{u}_0}{\partial x} - I_2\frac{\partial^2\ddot{w}_b}{\partial x^2} - J_2\frac{\partial^2\ddot{w}_s}{\partial x^2}\end{aligned} \tag{36}$$

$$\begin{aligned}&B_{11}^s\frac{\partial^3 u_0}{\partial x^3} - D_{11}^s\frac{\partial^4 w_b}{\partial x^4} - H_{11}^s\frac{\partial^4 w_s}{\partial x^4} + A_{55}^s\frac{\partial^2 w_s}{\partial x^2} \\ &= I_0(\ddot{w}_b+\ddot{w}_s) + J_1\frac{\partial\ddot{u}_0}{\partial x} - J_2\frac{\partial^2\ddot{w}_b}{\partial x^2} - K_2\frac{\partial^2\ddot{w}_s}{\partial x^2}\end{aligned} \tag{37}$$

Table 1 The admissible functions for distinct BCs

S-S	$X_n(x) = sin(\beta_n x), \beta_n = n\frac{\pi}{L}, n = 1,2,\ldots$
C-C	$X_n(x) = sin(\beta_n x) - sinh(\beta_n x) - \psi_n[cos(\beta_n x) - cosh(\beta_n x)]$ $\psi_n = [sin(\beta_n L) - sinh(\beta_n L)]/[cos(\beta_n L) - cosh(\beta_n L)]$ $\beta_n = \frac{(n+0.5)}{L}\pi$
C-S	$X_n(x) = sin(\beta_n x) - sinh(\beta_n x) - \psi_n[cos(\beta_n x) - cosh(\beta_n x)]$ $\psi_n = [sin(\beta_n L) + sinh(\beta_n L)]/[cos(\beta_n L) + cosh(\beta_n L)]$ $\beta_n = \frac{(n+0.25)}{L}\pi$
S-F	$X_n(x) = sin(\beta_n x) - sinh(\beta_n x) - \psi_n[cos(\beta_n x) - cosh(\beta_n x)]$ $\psi_n = [sin(\beta_n L) - sinh(\beta_n L)]/[cos(\beta_n L) - cosh(\beta_n L)]$ $\beta_1 = \frac{1.875}{L}, \beta_2 = \frac{4.694}{L}, \beta_3 = \frac{7.855}{L}, \beta_4 = \frac{10.966}{L},$ $\beta_n = \frac{(n-0.25)}{L}\pi \text{for} n \geq 5$

Table 2 The efficiency parameters of CNTs

	V_{cnt}^*		
	0.12	0.17	0.28
η_1	0.137	0.142	0.141
η_2	1.022	1.626	1.585
η_3	0.715	1.138	1.109

where A_{11}, B_{11}, D_{11}, B_{11}^s, D_{11}^s, H_{11}^s are the stiffnesses of the CNTRC beam given by:

$$(A_{11}, B_{11}, D_{11}, B_{11}^s, D_{11}^s, H_{11}^s) = \int_{-\frac{h}{2}}^{\frac{h}{2}} Q_{11}(1, z, z^2, f(z), z\,f(z), f^2(z))dz \tag{38}$$

$$A_{55}^s = \int_{-\frac{h}{2}}^{\frac{h}{2}} Q_{55}[g(z)]^2 dz \tag{39}$$

4. Analytical solution

It is possible to develop a closed-form solution for CNTRC beams under different BCs. To do this, the following BCs are considered for the arbitrary ends of the CNTRC beam:

Simply supported (S) ends:
$$w_b = w_s = 0 \text{ at } x = 0, L \tag{40}$$

Clamped (C) ends:
$$u_0 = w_b = \frac{\partial w_b}{\partial x} = w_s = \frac{\partial w_s}{\partial x} = 0 \text{ at } x = 0, L \tag{41}$$

Free (F) ends:
$$N_x = \frac{\partial M_x}{\partial x} = Q_x = M_x = 0 \text{ at } x = 0, L \tag{42}$$

The solution of the displacements that meet the BCs can be defined as:

$$\begin{Bmatrix} u_0 \\ w_b \\ w_s \end{Bmatrix} = \begin{Bmatrix} U_n X_n' e^{i\,\omega\,t} \\ W_{bn} X_n e^{i\,\omega\,t} \\ W_{sn} X_n e^{i\,\omega\,t} \end{Bmatrix} \tag{43}$$

where, U_n, W_{bn} and W_{sn} are random parameters to be determined, ω is the eigenfrequency linked with the m[th] eigenmode. Table 1 lists the functions that fulfil at least the geometric BCs provided in Eqs. (40)-(42), and represents approximately deflected CNTRC beam forms that were proposed by Reddy (2003a, b).

The analytical solutions may be found by inserting the Eqs. (43) into Eqs. (35)-(37)

$$\left(\begin{bmatrix} a_{11} & a_{12} & a_{13} \\ a_{21} & a_{22} & a_{23} \\ a_{31} & a_{32} & a_{33} \end{bmatrix} - \omega^2 \begin{bmatrix} m_{11} & m_{12} & m_{13} \\ m_{21} & m_{22} & m_{23} \\ m_{31} & m_{32} & m_{33} \end{bmatrix} \right) \begin{Bmatrix} U_m \\ W_{bm} \\ W_{sm} \end{Bmatrix} = \begin{Bmatrix} 0 \\ 0 \\ 0 \end{Bmatrix} \tag{44}$$

$$\begin{aligned} a_{11} &= \int_0^L A_{11} X''' X' dx, a_{12} = \int_0^L -B_{11} X''' X' dx, a_{13} = \int_0^L -B_{11}^s X''' X' dx, \\ a_{21} &= \int_0^L B_{11} X'''' X dx, a_{22} = \int_0^L -D_{11} X'''' X dx, a_{23} = \int_0^L -D_{11}^s X'''' X dx \\ a_{31} &= \int_0^L B_{11}^s X'''' X dx, a_{32} = \int_0^L -D_{11}^s X'''' X dx, a_{33} = \int_0^L (-H_{11}^s X'''' + A_{55}^s X'') X dx \end{aligned} \tag{45}$$

$$\begin{aligned} m_{21} &= -I_1 \int_0^L X'' X dx, m_{22} = -\int_0^L (I_0 X - I_2 X'') X dx, \\ m_{23} &= -\int_0^L (I_0 X + J_2 X'') X dx \\ m_{31} &= -J_1 \int_0^L X'' X dx, m_{32} = -\int_0^L (I_0 X - J_2 X'') X dx, \\ m_{33} &= -\int_0^L (I_0 X - K_2 X'') X dx \end{aligned} \tag{46}$$

5. Numerical results and discussions

This section compares and analyzes parametrical studies on the influences of L and NL CNT reinforcement on the NFs of CNTRC beams with various distribution patterns under four different BCs. In comparison studies, material and beam properties are taken from the related studies; however, in the whole paper, the efficiency parameters of CNTs based on the results of molecular dynamics simulations (Griebel and Hamaekers 2004, Han and Elliot 2007) are considered as in Table 2 (Shen and Xiang 2012).

5.1 Comparison studies

In this subsection, comparisons are carried out to demonstrate the validity of the existing formulations. It

Table 3 The comparisons of the first three DNFs of the CNTRC beams under various BCs versus distinct distribution patterns

BC	Modes	CNT-Pattern									
		UD		FG-Λ		FG-V		FG-X		FG-O	
		Shi *et al*. (2017)	Present	Shi *et al*. (2017)	Present	Shi *et al*. (2017)	Present	Shi *et al*. (2017)	Present	Shi *et al*. (2017)	Present
C-C	1	14.2538	16.0219	13.8550	15.4461	13.8550	15.4461	14.6267	16.6452	13.4354	14.1893
	2	28.5113	33.4284	27.9120	32.7346	27.9120	32.7346	29.1546	34.5598	27.3180	29.8507
	3	44.3037	52.1122	43.7355	51.4149	43.7355	51.4149	44.9606	54.0769	43.0775	46.0045
S-S	1	11.3232	11.5514	11.1214	10.5319	11.1214	10.5319	12.3011	12.5214	9.4702	9.5041
	2	27.9037	28.7233	26.8855	27.6618	26.8855	27.6618	28.8111	29.8562	25.9048	25.4040
	3	44.0270	46.7449	43.3760	45.8197	43.3760	45.8197	44.7878	48.3355	42.4459	41.7032

Table 4 The comparisons of the fundamental DNFs of the CNTRC beams under various BCs versus distinct values of L/h

B.C.	L/h	UD		FG-Λ		FG-O		FG-X	
		Ansari *et al*. (2014)	Present	Ansari *et al*. (2014)	Present	Ansari *et al*. (2014)	Present	Ansari *et al*. (2014)	Present
C-C	10	1.3650	1.5446	1.3283	1.4910	1.2892	1.3703	1.3997	1.6029
	12	1.3266	1.4818	1.2774	1.4147	1.2279	1.2987	1.3715	1.5476
	14	1.2850	1.4222	1.2239	1.3427	1.1654	1.2288	1.3403	1.4968
	16	1.2415	1.3643	1.1698	1.2740	1.1039	1.1614	1.3067	1.4479
	20	1.1526	1.2532	1.0643	1.1471	0.9884	1.0372	1.2352	1.3529
	30	0.9469	1.0135	0.8414	0.8940	0.7602	0.7959	1.0548	1.1347
C-S	10	1.2159	1.3813	1.1561	1.3040	1.1011	1.1933	1.2729	1.4538
	12	1.1564	1.3030	1.0852	1.2116	1.0219	1.1027	1.2236	1.3877
	14	1.0977	1.2278	1.0170	1.1259	0.9477	1.0189	1.1744	1.3233
	16	1.0407	1.1563	0.9528	1.0472	0.8796	0.9427	1.1256	1.2605
	20	0.9344	1.0265	0.8380	0.9109	0.7621	0.8130	1.0313	1.1420
	30	0.7231	0.7803	0.6271	0.6714	0.5579	0.5917	0.8282	0.8988
S-S	10	1.0901	1.1205	0.9941	1.0241	0.9150	0.9256	1.1822	1.2111
	12	0.9966	1.0274	0.8934	0.9231	0.8124	0.8284	1.0998	1.1283
	14	0.9122	0.9430	0.8065	0.8357	0.7266	0.7456	1.0216	1.0504
	16	0.8371	0.8677	0.7321	0.7605	0.6549	0.6753	0.9493	0.9783
	20	0.7130	0.7422	0.6140	0.6400	0.5439	0.5646	0.8239	0.8525
	30	0.5102	0.5342	0.4309	0.4512	0.3774	0.3948	0.6046	0.6297

should be noted that since there is not any available result for the free vibration of CNTRC beams with NL variation of volume fraction of CNTs, the validation studies are performed for those having L variation.

In Table 3, the comparison of the first three DNFs for CNTRC beams with distinct CNT distribution patterns under C-C and S-S BCs with the results of Shi *et al*. (2017) is presented. The material and beam properties are taken from the study of Shi *et al*. (2017) as: $k = 1, \frac{L}{h} = 10$, $V_{cnt}^{*} = 0.12$, $E^{p} = 2.5\text{GPa}$, $\rho^{p} = 1150\text{kg/m}^3$, $\nu^{p} = 0.3$, $E_{11}^{cnt} = 5646.6\text{GP}$, $E_{22}^{cnt} = 7080\text{GPa}$, $G_{12}^{cnt} = 1944.5$ GPa, $\nu^{cnt} = 0.175$, and $\rho^{cnt} = 2100\text{kg/m}^3$ P, and Besides, the dimensionless natural frequencies (DNFs) are defined as: $\Omega = \omega L^2 \sqrt{\frac{\rho^{p}}{(E^{p}h^2)}}$. Minor differences are observed between the results, especially in the higher modes and high values of NFs for C-C boundary conditions since Shi *et al*. (2017) used the FSDT and strong-form solution procedure of the modified Fourier method for the formulation and solution of the problem, respectively. It is noted that although FG-Λ and FG-V are two different distribution patterns, they both give the same results. Therefore, one of these distribution patterns will be considered in the subsequent analyzes of the present paper.

In Table 4, the comparison of the fundamental DNFs for CNTRC beams with different values of specified CNT volume fraction under four different BCs with the results of Ansari *et al*. (2014) is made. The material properties are taken from the study of Ansari *et al*. (2014) as: $k = 1, V_{cnt}^{*} = 0.12, E^{p} = 2.5\text{GPa}$, $\rho^{p} = 1150\text{kg/m}^3$, $\nu^{p} = 0.34$,

Table 5 The variation of the first three DNFs of the CNTRC beams under various BCs versus distinct values of k

Mode	S-S												
	UD	FG-O				FG-X				FG-Λ			
	k	k				k				k			
	0	0.5	1	2.	4	0.5	1	2.	4	0.5	1	2.	4
1	1.1055	0.9971	0.9096	0.7767	0.6089	1.1634	1.1983	1.2403	1.2839	1.0552	1.0080	0.9234	0.7896
2	2.7487	2.5699	2.4311	2.2209	1.9310	2.8155	2.8571	2.9076	2.9593	2.6835	2.6472	2.5936	2.4602
3	4.4733	4.1895	3.9908	3.7305	3.4254	4.5675	4.6255	4.6870	4.7267	4.3911	4.3848	4.4162	4.4042
Mode	C-C												
	UD	FG-O				FG-X				FG-Λ			
	k	k				k				k			
	0	0.5	1	2.	4	0.5	1	2.	4	0.5	1	2.	4
1	1.5330	1.4343	1.3579	1.2426	1.0840	1.5700	1.5929	1.6207	1.6490	1.4975	1.4782	1.4506	1.3814
2	3.1989	2.9982	2.8566	2.6684	2.4433	3.2659	3.3072	3.3520	3.3835	3.1396	3.1326	3.1494	3.1324
3	4.9870	4.6347	4.4023	4.1334	3.8874	5.1056	5.1750	5.2364	5.2437	4.8987	4.9203	5.0172	5.1065
Mode	C-S												
	UD	FG-O				FG-X				FG-Λ			
	k	k				k				k			
	0	0.5	1	2.	4	0.5	1	2.	4	0.5	1	2.	4
1	1.3682	1.2634	1.1783	1.0453	0.8642	1.4147	1.4429	1.4775	1.5145	1.3244	1.2891	1.2268	1.1089
2	2.9825	2.7970	2.6596	2.4632	2.2048	3.0467	3.0868	3.1336	3.1759	2.9217	2.9009	2.8845	2.8116
3	4.7298	4.4161	4.2036	3.9427	3.6701	4.8340	4.8967	4.9576	4.9823	4.6457	4.6536	4.7190	4.7621
Mode	C-F												
	UD	FG-O				FG-X				FG-Λ			
	k	k				k				k			
	0	0.5	1	2.	4	0.5	1	2.	4	0.5	1	2.	4
1	0.5610	0.4743	0.4117	0.3279	0.2387	0.6245	0.6662	0.7181	0.7703	0.5154	0.4711	0.4002	0.3137
2	1.5263	1.4277	1.3514	1.2363	1.0778	1.5630	1.5859	1.6137	1.6420	1.4906	1.4712	1.4432	1.3736
3	3.1994	2.9987	2.8570	2.6688	2.4437	3.2664	3.3077	3.3526	3.3841	3.1401	3.1331	3.1499	3.1329

$E_{11}^{cnt} = 5646.6$GPa, $E_{22}^{cnt} = 7080$GPa $E_{22}^{cnt} = 7080$GPa, $G_{12}^{cnt} = 1944.5$GPa, $\nu^{cnt} = 0.175$, and $\rho^{cnt} = 1400\,\text{kg/m}^3$. Besides, the DNF is defined as: $\Omega = \omega L\sqrt{\frac{I_{10}}{A_{110}}}$. Because Ansari *et al*. (2014) adopted FSDT to formulate the problem, slight differences are observed between both results in Table 4, especially in the high values of NFs for C-C boundary conditions.

Therefore, the results obtained and reported in Tables 3 and 4 are consistent with those available in the literature, and these findings verify the correctness of the present formulation.

5.2 Parametrical studies

This subsection presents parametrical studies on the influences of NL-CNT reinforcement on the NFs of CNTRC beams having UD, FGΛ, FG-O, and FG-X distribution patterns. In this research, the matrix and reinforcing material are assumed to be polymethyl methacrylate (PMMA), and the armchair (10,10) SWCNTs, respectively, and the following values for the numerical analyzes are considered unless otherwise stated (Shen and Xiang 2012): $E^p = 2.5$GPa, $\rho^p = 1190\text{kg/m}^3$, $\nu^p = 0.3$, $E_{11}^{cnt} = 5646.6$GPa, $E_{22}^{cnt} = 7080$GPa, $G_{12}^{cnt} = 1944.5$GPa, $\nu^{cnt} = 0.175$, and $\rho^{cnt} = 2100\text{kg/m}^3$. Moreover, unless otherwise stated in the numerical examples, DNF is denoted: $\Omega = \omega L\sqrt{\frac{I_{10}}{A_{110}}}$. Here A_{110} and I_{10} are the stiffness and mass moment of inertia of CNTRC beam composed of the pure matrix material, respectively.

Study 1: First, the influence of NL variation of exponent of volume fraction of CNTs on the DNFs of CNTRC beam per the varying mode number is examined. To do this, Table 5 shows the interaction of both changes in the values of the exponent of volume fraction of CNTs (k) and the mode numbers (MNs) on the DNFs of the CNTRC beams having distinct distribution patterns under different BCs for $L/h = 10, V_{cnt}^* = 0.12$. The results highlighted that the influence of k on the values of the first three DNFs of CNTRC beams differs according to the chosen distribution pattern, MNs, and BCs. In the CNTRC beams having FG-O

Table 6 The fundamental DNFs of the CNTRC beams under various BCs versus distinct values of V_{cnt}^{*}

	S-S									
V_{CNT}^{*}	UD		FG-O		FG-X			FG-Λ		
	k		k		k			k		
	0	0.5	1	2	0.5	1	2	0.5	1	2
0.12	1.1055	0.9971	0.9096	0.7767	1.1634	1.1983	1.2403	1.0552	1.008	0.9234
0.17	1.3628	1.2258	1.1139	0.9425	1.4353	1.4781	1.5283	1.2967	1.2317	1.1134
0.28	1.5088	1.393	1.2928	1.1383	1.5574	1.5847	1.6162	1.4509	1.3909	1.2765
	C-C									
V_{CNT}^{*}	UD		FG-O		FG-X			FG-Λ		
	k		k		k			k		
	0	0.5	1	2	0.5	1	2	0.5	1	2
0.12	1.533	1.4343	1.3579	1.2426	1.57	1.5929	1.6207	1.4975	1.4782	1.4506
0.17	1.9827	1.8072	1.7126	1.5651	1.9647	1.9887	2.017	1.8788	1.8477	1.7952
0.28	2.1096	1.9664	1.9108	1.8748	2.0564	2.0637	2.0718	2.0132	1.9943	1.9660
	C-S									
V_{CNT}^{*}	UD		FG-O		FG-X			FG-Λ		
	k		k		k			k		
	0	0.5	1	2	0.5	1	2	0.5	1	2
0.12	1.3682	1.2634	1.1783	1.0453	1.4147	1.4429	1.4775	1.3244	1.2891	1.2268
0.17	1.7064	1.5759	1.4671	1.2932	1.7621	1.7948	1.8336	1.6485	1.5967	1.5008
0.28	1.8397	1.7449	1.6653	1.5554	1.8648	1.8795	1.897	1.795	1.7541	1.6763
	C-F									
V_{CNT}^{*}	UD		FG-O		FG-X			FG-Λ		
	k		k		k			k		
	0	0.5	1	2	0.5	1	2	0.5	1	2
0.12	0.561	0.4743	0.4117	0.3279	0.6245	0.6662	0.7181	0.5154	0.4711	0.4002
0.17	0.669	0.5642	0.4883	0.3865	0.7458	0.796	0.8582	0.6133	0.5586	0.4704
0.28	0.8036	0.682	0.5921	0.4696	0.8892	0.9438	1.0101	0.7385	0.6734	0.5662

distribution pattern, the DNFs decrease noticeably with the increase of the k, whereas in CNTRC beams having FG-X distribution pattern, the DNFs increase with the increase of the k, for all cases examined. However, in CNTRC beams having FG-Λ distribution pattern, the DNFs decrease with the rise of k in the first mode; then, it remains almost constant in the other modes in all cases examined. Compared to the other two distribution patterns, the FG-O pattern has greater sensitivity to variation of *k*. In addition, the variation of the k has the more significant influence on the fundamental mode and losses its efficiency with the increase of the MNs. Furthermore, the variation of the k has the greatest influence on C-F BCs, whereas it has the lowest influence on the C-C BCs.

Study 2: Secondly, the influence of NL variation of exponent of volume fraction of CNTs on the fundamental DNFs of CNTRC beam by the change of specified volume fraction is analyzed. For this objective, Table 6 presents the relationships of the changes in the values of k and specified volume fractions, V_{cnt}^{*}, on the fundamental DNFs of the CNTRC beams having distinct distribution patterns under different BCs for $L/h = 10$. The values of DNFs of the CNTRC beams increase with the increasing of V_{cnt}^{*}, in all cases. The results indicate that the influence of k on the values of the fundamental DNFs of the CNTRC beams varies corresponding to the chosen distribution pattern, specified volume fraction, and BCs. The influence of the variation of k on the values of the fundamental DNFs changes irregularly for the different values of V_{cnt}^{*}. In summary, the highest influence occurs in the FG-O distribution pattern under C-F BCs, whereas the lowest influence arises in the FG-X distribution pattern under C-C BCs for $V_{cnt}^{*} = 0.17$.

Study 3: Thirdly, the influence of NL variation of exponent of volume fraction of CNTs on the fundamental DNFs of CNTRC beam versus the varying span-to-depth ratio is investigated. For this purpose, Table 7 demonstrates the mutual effect of the change in the values of k and span-to-depth ratio, L/h, on the fundamental DNFs of the CNTRC beams having distinct distribution patterns under

Table 7 The fundamental DNFs of the CNTRC beams under various BCs versus distinct values of L/h

L/h	S-S									
	UD	FG-O			FG-X			FG-Λ		
	k	k			k			k		
	0	1	2	4	1	2	4	1	2	4
10	1.1055	0.9096	0.7767	0.6089	1.1983	1.2403	1.2839	1.0080	0.9234	0.7896
15	0.8876	0.6934	0.5717	0.4305	0.9982	1.0490	1.1002	0.7803	0.6895	0.5640
20	0.7262	0.5508	0.4463	0.3302	0.8367	0.8888	0.9410	0.6252	0.5423	0.4346
L/h	C-C									
	UD	FG-O			FG-X			FG-Λ		
	k	k			k			k		
	0	1	2	4	1	2	4	1	2	4
10	1.5332	1.3579	1.2426	1.0840	1.5929	1.6207	1.6490	1.4782	1.4506	1.3814
15	1.3790	1.1787	1.0384	0.8494	1.4606	1.4981	1.5382	1.2921	1.2214	1.0929
20	1.2366	1.0195	0.8718	0.6848	1.3389	1.3851	1.4333	1.1292	1.0365	0.8889
L/h	C-S									
	UD	FG-O			FG-X			FG-Λ		
	k	k			k			k		
	0	1	2	4	1	2	4	1	2	4
10	1.3682	1.1783	1.0453	0.8642	1.4429	1.4775	1.5145	1.2891	1.2268	1.1089
15	1.1751	0.9625	0.8190	0.6395	1.2776	1.3239	1.3720	1.0681	0.9754	0.8308
20	1.0086	0.7958	0.6602	0.5005	1.1258	1.1793	1.2334	0.8930	0.7944	0.6549
L/h	C-F									
	UD	FG-O			FG-X			FG-Λ		
	k	k			k			k		
	0	1	2	4	1	2	4	1	2	4
10	0.5610	0.4117	0.3279	0.2387	0.6662	0.7181	0.7703	0.4711	0.4002	0.3137
15	0.3864	0.2801	0.2218	0.1605	0.4645	0.5038	0.5436	0.3218	0.2718	0.2120
20	0.2933	0.2116	0.1672	0.1208	0.3543	0.3852	0.4167	0.2435	0.2052	0.1598

different BCs for $V_{cnt}^{*} = 0.12$. The values of DNFs of the CNTRC beams decrease with the growth of L/h, in all cases. On the other hand, the influence of the variation of k on the values of the fundamental DNFs increases with the increase of the values of L/h, in all cases. The results imply that the influence of k on the values of the fundamental DNFs of the CNTRC beams varies corresponding to the chosen distribution pattern, span-to-depth ratio, and BCs. In a nutshell, the greatest influence happens in the FG-O distribution pattern under C-F BCs, whereas the lowest influence develops in the FG-X distribution pattern under C-C BCs.

6. Conclusions

In this paper, the influences of the variation of the exponent of volume fraction of CNTs on the NFs of the CNTRC beams were investigated under different BCs employing TSDT. The mixture rule was applied to determine the mechanical properties of the CNTRC beams. The equations of motion were found using Hamilton's principle. Under four different BCs, the resulting equations are solved analytically. The impacts of the variation of exponent of CNT volume fraction and its interaction with the types of CNT distribution patterns, span-to-depth ratio, and BCs on the NFs of the CNTRC beams were studied comprehensively in the numerical examples.

In conclusion, the research outcomes are:

• The NL variation of k has the highest impact on the fundamental DNFs of the CNTRC beams

• The NL variation of k has the highest impact on the DNFs of the CNTRC beams having FG-O distribution patterns

• The NL variation of k has the lowest impact on the DNFs of the CNTRC beams having FG-X distribution patterns

• The NL variation of k has the highest impact on the DNFs of the CNTRC beams under C-F BCs

• The NL variation of k has the lowest impact on the DNFs of the CNTRC beams under C-C BCs

• The NL variation of k has an irregular impact on the

fundamental DNFs of the CNTRC beams for the different values of V_{cnt}^{*}.

Consequently, it is discovered that the change in the exponent of the volume fraction of the CNTs, as well as its interaction with the types of CNT distribution patterns, span-to-depth ratio, and BCs, have significant influences on the natural frequencies of the CNTRC beams. Therefore, designers, researchers, scientists, and engineers working with the CNTRC beams may find this study helpful in deciding the needed NF by varying the range of factors examined here. Besides, the created model is noteworthy for not only addressing the influence of the shear deformation but also for dealing with only three unknowns, as opposed to the FSDT of Timoshenko, which includes a shear correction factor. Therefore, the applied theory not only solved the current problem and generated well outcomes but also simplified the vibration analysis of the CNTRC beams. In the future, the present research will be broadened to incorporate mechanical features of various types of structures made up of various materials with micro/macro sizes.

References

Afshin, S. and Yas, M.H. (2020), "Dynamic and buckling analysis of polymer hybrid composite beam with variable thickness", *Appl. Math. Mech.*, **41**, 785-804. https://doi.org/10.1007/S10483-020-2610-7

Alibeigloo, A. and Emtehani, A. (2015), "Static and free vibration analyzes of carbon nanotube-reinforced composite plate using differential quadrature method", *Meccanica*, **50**, 61-76. https://doi.org/10.1007/S11012-014-0050-7

Ansari, R., Faghih Shojaei, M., Mohammadi, V., Gholami R. and Sadeghi, F. (2014), "Nonlinear forced vibration analysis of functionally graded carbon nanotube-reinforced composite Timoshenko beams", *Compos. Struct.*,**113**, 316-327. https://doi.org/10.1016/j.compstruct.2014.03.015

Ansari, R., Torabi, J. and Hassani, R. (2019), "A comprehensive study on the free vibration of arbitrary shaped thick functionally graded CNT-reinforced composite plates", *Eng. Struct.*, **181**, 653-669. https://doi.org/10.1016/j.engstruct.2018.12.049

Arani, A. G., Kolahchi, R. and Esmailpour, M. (2016), "Nonlinear vibration analysis of piezoelectric plates reinforced with carbon nanotubes using DQM", *Smart Struct. Syst., Int. J.*, **18**(4), 787-800. https://doi.org/10.12989/sss.2016.18.4.787

Barretta R., Caporale A., Faghidian S.A., Luciano R., Marotti de Sciarra F. and Medaglia C. M. (2019), "A stress-driven local-nonlocal mixture model for Timoshenko nano-beams", *Compos. Part B Eng.*, **164**, 590-598. https://doi.org/10.1016/j.compositesb.2019.01.012

Benachour, A., Tahar, H.D., Atmane, H.A., Tounsi, A. and Ahmed, M.S. (2011), "A four variable refined plate theory for free vibrations of functionally graded plates with arbitrary gradient", *Compos. Part B Eng.* **42**, 1386-1394. https://doi.org/10.1016/j.compositesb.2011.05.032

Bisheh, H., Wu, N. and Rabczuk, T. (2020), "Free vibration analysis of smart laminated carbon nanotube-reinforced composite cylindrical shells with various boundary conditions in hygrothermal environments", *Thin Walled Struct.*, **149**, 106500. https://doi.org/10.1016/J.TWS.2019.106500

Borjalilou, V., Taati, E. and Ahmadian, M.T. (2019), "Bending, buckling and free vibration of nonlocal FG-carbon nanotube-reinforced composite nanobeams: exact solutions", *SN Appl. Sci.*, **1**, 1323. https://doi.org/10.1007/S42452-019-1359-6

Bousahla, A.A., Bourada, F., Mahmoud, S.R., Tounsi, A., Algarni, A., Adda Bedia, E.A. and Tounsi, A. (2020), "Buckling and dynamic behavior of the simply supported CNT-RC beams using an integral-first shear deformation theory", *Comput. Concr.*, **25**, 155-166. https://doi.org/10.12989/cac.2020.25.2.155

Chamran, S., Chen, C.-S., Fung, C.-P., Wang, H. and Chen, W.-R. (2022), "Dynamic response of functionally graded carbon nanotube-reinforced hybrid composite plates", *J. Appl. Comput. Mech.*, **8**, 182-195. https://doi.org/10.22055/JACM.2021.37884.3108

Chiroiu, V., Munteanu, L. and Gliozzi, A.S. (2010), "Application of cosserat theory to the modelling of reinforced carbon nananotube beams", *Comput. Mater. Contin.*, **19**, 1-16. https://doi.org/10.3970/cmc.2010.019.001

Civalek, Ö. and Avcar, M. (2020), "Free vibration and buckling analyzes of CNT reinforced laminated non-rectangular plates by discrete singular convolution method", *Eng. Comput.* **1**, 1-33. https://doi.org/10.1007/s00366-020-01168-8

Civalek, Ö. and Baltacıoğlu, A.K. (2018), "Vibration of carbon nanotube reinforced composite (CNTRC) annular sector plates by discrete singular convolution method", *Compos. Struct.*, **203**, 458-465. https://doi.org/10.1016/j.compstruct.2018.07.037

Deepak, B.P., Ganguli, R. and Gopalakrishnan, S. (2012), "Dynamics of rotating composite beams: A comparative study between CNT reinforced polymer composite beams and laminated composite beams using spectral finite elements", *Int. J. Mech. Sci.*, **64**, 110-126. https://doi.org/10.1016/j.ijmecsci.2012.07.009

Ehyaei, J. and Daman, M. (2017), "Free vibration analysis of double walled carbon nanotubes embedded in an elastic medium with initial imperfection", *Adv. Nano Res.*, **5**(2), 179. https://doi.org/10.12989/anr.2017.5.2.179

El-Ashmawy, A.M. and Xu, Y. (2021), "Combined effect of carbon nanotubes distribution and orientation on functionally graded nano-composite beams using finite element analysis" *Mater. Res. Express*, **8**. https://doi.org/10.1088/2053-1591/ABC773

Esawi, A.M.K. and Farag, M.M. (2007), "Carbon nanotube reinforced composites: potential and current challenges", *Mater. Des.*, **28**, 2394-2401. https://doi.org/10.1016/j.matdes.2006.09.022

Feng, T., Liu, N., Wang, S., Qin, C., Shi, S., Zeng, X. and Liu, G. (2021), "Research on the dispersion of carbon nanotubes and their application in solution-processed polymeric matrix composites: A review", *Adv. Nano Res.*, **10**(6), 559-576. https://doi.org/10.12989/anr.2021.10.6.559

Griebel, M. and Hamaekers, J. (2004), "Molecular dynamics simulations of the elastic moduli of polymer-carbon nanotube composites", *Comput. Methods Appl. Mech. Eng.*, **193**, 1773-1788. https://doi.org/10.1016/j.cma.2003.12.025

Han, Y. and Elliott, J. (2007), "Molecular dynamics simulations of the elastic properties of polymer/carbon nanotube composites", *Comput. Mater. Sci.*, **39**, 315-323. https://doi.org/10.1016/j.commatsci.2006.06.011

Hedayati, H. and Sobhani Aragh, B. (2012), "Influence of graded agglomerated CNTs on vibration of CNT-reinforced annular sectorial plates resting on Pasternak foundation", *Appl. Math. Comput.*, **218**, 8715-8735. https://doi.org/10.1016/J.AMC.2012.01.080

Heshmati M. and Yas M. H. (2013), "Free vibration analysis of functionally graded CNT-reinforced nano-composite beam using Eshelby-Mori-Tanaka approach", *J. Mech. Sci. Technol.*, **27**, 3403-3408. https://doi.org/10.1007/S12206-013-0862-8

Heshmati, M., Yas, M.H. and Daneshmand, F. (2015), "A comprehensive study on the vibrational behavior of CNT-reinforced composite beams", *Compos. Struct.*, **125**, 434-448. https://doi.org/10.1016/j.compstruct.2015.02.033

Hussain, M., Naeem, M. N., Asghar, S., & Tounsi, A. (2020), "Theoretical impact of Kelvin's theory for vibration of double walled carbon nanotubes", *Adv. Nano Res.*, **8**(4), 307-322. https://doi.org/10.12989/anr.2020.8.4.307

Iijima S. (1991), "Helical microtubules of graphitic carbon", Nature, **354**, 56-58. https://doi.org/10.1038/354056a0

Jalaei, M.H., Thai, H.T. and Civalek, O. (2022), "On viscoelastic transient response of magnetically imperfect functionally graded nanobeams", *Int. J. Eng. Sci.*, **172**, 103629. https://doi.org/10.1016/j.ijengsci.2022.103629

Jam, J.E. and Kiani, Y. (2015), "Buckling of pressurized functionally graded carbon nanotube reinforced conical shells", *Compos. Struct.*, **125**, 586-595. https://doi.org/10.1016/j.compstruct.2015.02.052

Kamarian, S., Salim, M., Dimitri, R. and Tornabene, F. (2016), "Free vibration analysis of conical shells reinforced with agglomerated Carbon Nanotubes", *Int. J. Mech. Sci.*, **108-109**, 157-165. https://doi.org/10.1016/j.ijmecsci.2016.02.006

Kamarian, S., Shakeri, M., Karimi, B. and Pourasghar, A. (2016), "Free vibration analysis and design optimization of nanocomposite-laminated beams using various higher order beam theories and imperialist competitive algorithm", *Polym. Compos.*, **37**, 2442-2451. https://doi.org/10.1002/PC.23429

Kaw, A. (2006), *Mechanics Composite of Materials*, CRC Press, Boca Raton.

Ke L.L., Yang J. and Kitipornchai S. (2010), "Nonlinear free vibration of functionally graded carbon nanotube-reinforced composite beams", *Compos. Struct.*, **92**, 676-683. https://doi.org/10.1016/j.compstruct.2009.09.024

Khadimallah, M.A., Hussain, M., Taj, M., Ayed, H. and Tounsi, A. (2021), "Parametric vibration analysis of single-walled carbon nanotubes based on Sanders shell theory", *Adv. Nano Res.*, **10**(2), 165-174. https://doi.org/10.12989/anr.2021.10.2.165

Khadir, A.I., Daikh, A.A. and Eltaher, M.A. (2021), "Novel four-unknowns quasi 3D theory for bending, buckling and free vibration of functionally graded carbon nanotubes reinforced composite laminated nanoplates", *Adv. Nano Res.*, **11**(6), 621-640. https://doi.org/10.12989/anr.2021.11.6.621

Khilari, S., Kochar, S., Sanvordenker, R. and Thomas B. (2018), "Free vibration analysis of carbon nanotube reinforced composite Timoshenko beam", *Prog. Ind. Ecol.*, **12**, 78-92. https://doi.org/10.1504/PIE.2018.095873

Kumar, P. and Srinivas, J. (2017), "Free vibration, bending and buckling of a FG-CNT reinforced composite beam Comparative analysis with hybrid laminated composite beam", *Multidiscipl. Model. Mater. Struct.*, **13**, 590-611. https://doi.org/10.1108/MMMS-05-2017-0032

Lau, K.T., Gu, C., Gao, G.H., Ling, H.Y. and Reid, S.R. (2004), "Stretching process of single- and multi-walled carbon nanotubes for nano-composite applications", *Carbon N. Y.*, **42**, 426-428. https://doi.org/10.1016/j.carbon.2003.10.040

Lau, A.K.T. and Hui, D. (2002), "The revolutionary creation of new advanced materials - Carbon nanotube composites", *Compos. Part B Eng.*, **33**, 263-277. https://doi.org/10.1016/S1359-8368(02)00012-4

Liew, K.M., Lei, Z.X. and Zhang, L.W. (2015), "Mechanical analysis of functionally graded carbon nanotube reinforced composites: A review", *Compos. Struct.* **120**, 90-97. https://doi.org/10.1016/j.compstruct.2014.09.041

Lin, F. and Xiang, Y. (2014a), "Numerical analysis on nonlinear free vibration of carbon nanotube reinforced composite beams", *Int. J. Struct. Stab. Dyn.* **14**, 1350056. https://doi.org/10.1142/S0219455413500569

Lin, F. and Xiang, Y. (2014b), "Vibration of carbon nanotube reinforced composite beams based on the first and third order beam theories", *Appl. Math. Model.*, **38**, 3741-3754. https://doi.org/10.1016/j.apm.2014.02.008

Loos, M. R. (2014), "Carbon Nanotube Reinforced Composites: CNR Polymer Science and Technology", *Carbon Nanotub. Reinf. Compos. CNR Polym. Sci. Technol.*, 1-289. https://doi.org/10.1016/C2012-0-06123-6

Mahmoodi, S.N., Jalili N. and Khadem S.E. (2005), "Passive nonlinear vibrations of a directly excited nanotube-reinforced composite cantilever beam", *Am. Soc. Mech. Eng. Dyn. Syst. Control Div. DSC 74 DSC*, 1913-1920. https://doi.org/10.1115/IMECE2005-81608

Mahmoodi, M.J., Maleki, M. and Hassanzadeh-Aghdam, M.K. (2018), "Static bending and free vibration analysis of hybrid fuzzy-fiber reinforced nano-composite beam-A multi-scale modeling", *Int. J. Appl. Mech.*, **10**. https://doi.org/10.1142/S1758825118500539

Mayandi, K. and Jeyaraj, P. (2015), "Bending, buckling and free vibration characteristics of FG-CNT-reinforced polymer composite beam under non-uniform thermal load", *Proc. Inst. Mech. Eng. Part L J. Mater. Des. Appl.*, **229**, 13-28. https://doi.org/10.1177/1464420713493720

Mohammadimehr, M. and Alimirzaei, S. (2017), "Buckling and free vibration analysis of tapered FG-CNTRC micro Reddy beam under longitudinal magnetic field using FEM", *Smart Struct. Syst.*, **19**, 309-322. https://doi.org/10.12989/SSS.2017.19.3.309

Mohammadimehr, M., Mohammadi-Dehabadi, A.A., Alavi, S.M.A., Alambeigi, K., Bamdad, M., Yazdani, R. and Hanifehlou, S. (2018), "Bending, buckling, and free vibration analyzes of carbon nanotube reinforced composite beams and experimental tensile test to obtain the mechanical properties of nano-composite", *Steel Compos. Struct.*, **29**, 405-422. https://doi.org/10.12989/SCS.2018.29.3.405

Mohammadimehr M., Monajemi A.A. and Afshari H. (2020), "Free and forced vibration analysis of viscoelastic damped FG-CNT reinforced micro composite beams", *Microsyst. Technol.*, **26**, 3085-3099. https://doi.org/10.1007/S00542-017-3682-4

Mohseni, A. and Shakouri, M. (2019), "Vibration and stability analysis of functionally graded CNT-reinforced composite beams with variable thickness on elastic foundation", *Proc. Inst. Mech. Eng. Part L J. Mater. Des. Appl.*, **233**, 2478-2489. https://doi.org/10.1177/1464420719866222

Moradi-Dastjerdi, R. and Payganeh, G. (2017), "Thermoelastic dynamic analysis of wavy carbon nanotube reinforced cylinders under thermal loads", *Steel Compos. Struct.*, **25**, 315-326. https://doi.org/10.12989/scs.2017.25.3.315

Nejadi, M.M., Mohammadimehr, M. and Mehrabi, M. (2021), "Free vibration and buckling of functionally graded carbon nanotubes/graphene platelets Timoshenko sandwich beam resting on variable elastic foundation", *Adv. Nano Res.*, **10**(6), 539-548. https://doi.org/10.12989/anr.2021.10.6.539

Nejati M., Eslampanah A. and Najafizadeh M. (2018), "Buckling and vibration analysis of functionally graded carbon nanotube-reinforced beam under axial load, *Int. J. Appl. Mech.*, **8**, 1650008. https://doi.org/10.1142/S1758825116500083

Rashad, A.M. (2017), "Effect of carbon nanotubes (CNTs) on the properties of traditional cementitious materials", *Constr. Build. Mater.*, **153**, 81-101. https://doi.org/10.1016/j.conbuildmat.2017.07.089

Ramezani, M., Kim, Y.H. and Sun, Z. (2021), "Elastic modulus formulation of cementitious materials incorporating carbon nanotubes: Probabilistic approach" *Constr. Build. Mater.*, **275**, 122092. https://doi.org/10.1016/j.conbuildmat.2020.122092

Ramezani, M., Dehghani, A. and Sherif, M. M. (2022), "Carbon nanotube reinforced cementitious composites: A comprehensive review", *Constr. Build. Mater.*, **315**, 125100. https://doi.org/10.1016/j.conbuildmat.2021.125100

Rezaiee-Pajand, M., Masoodi, A.R. and Rajabzadeh-Safaei, N. (2019), "Nonlinear vibration analysis of carbon nanotube

reinforced composite plane structures", *Steel Compos. Struct.*, **30**, 493-516. https://doi.org/10.12989/scs.2019.30.6.493

Reddy, J.N. (2003a), *Mechanics of Laminated Composite Plates and Shells*, CRC Press, Boca Raton. https://doi.org/10.1201/b12409

Reddy, J.N. (2003b), *Theory And Analysis Of Elastic Plates And Shells*, CRC Press, Boca Raton.

Saifuddin, N., Raziah, A.Z., Junizah, A.R. (2013), "Carbon nanotubes: A review on structure and their interaction with proteins", *J. Chem.*, 676815. https://doi.org/10.1155/2013/676815

Seidi, J. and Kamarian, S. (2017), "Free vibrations of non-uniform CNT/fiber/polymer nano-composite beams", *Curved Layer. Struct.*, **4**, 21-30. https://doi.org/10.1515/CLS-2017-0003

Shen, H.S. (2009), "Nonlinear bending of functionally graded carbon nanotube-reinforced composite plates in thermal environments", *Compos. Struct.*, **91**, 9-19. https://doi.org/10.1016/j.compstruct.2009.04.026

Shen, H.S. (2012), "Thermal buckling and postbuckling behavior of functionally graded carbon nanotube-reinforced composite cylindrical shells", *Compos. Part B Eng.* **43**, 1030-1038. https://doi.org/10.1016/j.compositesb.2011.10.004

Shen, H.S. and Xiang, Y. (2012), "Nonlinear vibration of nanotube-reinforced composite cylindrical shells in thermal environments" *Comput. Methods Appl. Mech. Eng.*, **213-216**, 196-205. https://doi.org/10.1016/J.CMA.2011.11.025

Shen, H.S. and Xiang, Y. (2013), "Nonlinear analysis of nanotube-reinforced composite beams resting on elastic foundations in thermal environments", *Eng. Struct.*, **56**, 698-708. https://doi.org/10.1016/j.engstruct.2013.06.002

Shi, Z., Yao, X., Pang, F. and Wang, Q. (2017), "An exact solution for the free-vibration analysis of functionally graded carbon-nanotube-reinforced composite beams with arbitrary boundary conditions", *Sci. Rep.*, **7**, 1-18. https://doi.org/10.1038/s41598-017-12596-w

Thomas B. and Suresh T.P. (2017), "Vibration and buckling analysis of functionally graded carbon nanotube reinforced composite beams", *Int. J. Civ. Eng. Technol.*, **8**, 74-84.

Tounsi, A., Benguediab, S., Semmah, A. and Zidour, M. (2013), "Nonlocal effects on thermal buckling properties of double-walled carbon nanotubes", *Adv. Nano Res.*, **1**(1), 1-11. https://doi.org/10.12989/anr.2013.1.1.001

Vinson, J.R. and Sierakowski R.L. (2008), *The Behavior of Structures Composed of Composite Materials* (*Solid Mechanics and its Applications)*, Kluwer Academic Publishers.

Vo-Duy, T., Ho-Huu, V. and Nguyen-Thoi, T. (2019), "Free vibration analysis of laminated FG-CNT reinforced composite beams using finite element method", *Front. Struct. Civil Eng.*, **13**, 324-336. https://doi.org/10.1007/S11709-018-0466-6

Wang, Z.X. and Shen, H.S. (2011), "Nonlinear vibration of nanotube-reinforced composite plates in thermal environments", *Comput. Mater. Sci.*, **50**, 2319-2330. https://doi.org/10.1016/j.commatsci.2011.03.005

Xu, J., Yang, Z., Yang, J. and Li, Y. (2021), "Free vibration analysis of rotating FG-CNT reinforced composite beams in thermal environments with general boundary conditions", *Aerosp. Sci. Technol.*, **118**. https://doi.org/10.1016/J.AST.2021.107030

Yang, J., Huang, X.H. and Shen, H.S. (2020), "Nonlinear flexural behavior of temperature-dependent FG-CNTRC laminated beams with negative Poisson's ratio resting on the Pasternak foundation", Eng. Struct. **207**, 110250. https://doi.org/10.1016/j.engstruct.2020.110250

Yas, M.H. and Samadi N. (2012), "Free vibrations and buckling analysis of carbon nanotube-reinforced composite Timoshenko beams on elastic foundation" *Int. J. Press. Vessel. Pip.*, **98**, 119-128. https://doi.org/10.1016/j.ijpvp.2012.07.012

Zerrouki, Rachid;Karas, Abdelkader;Zidour M. (2020), "Critical buckling analyzes of nonlinear FG-CNT reinforced nano-composite beam", *Adv. Nano Res.*, **9**(3), 211-220. https://doi.org/10.12989/anr.2020.9.3.211

Zerrouki, R., Karas, A., Zidour, M., Bousahla, A.A., Tounsi, A., Bourada, F., Tounsi, A., Benrahou, K.H. and Mahmoud S.R. (2021), "Effect of nonlinear FG-CNT distribution on mechanical properties of functionally graded nano-composite beam", *Struct. Eng. Mech.*, **78**, 117-124. https://doi.org/10.12989/sem.2021.78.2.117

CC